Progress In Electromagnetics Research C, Vol. 150, 187-193, 2024 PIER C

(Received 8 October 2024, Accepted 26 November 2024, Scheduled 5 December 2024)

A Miniaturized Tri-Band CP Antenna

Gaurav Kumar*, Pratik Mevada, Ramesh C. Gupta, Vijay K. Singh, Sanjeev Kulshrestha, and Milind B. Mahajan

Space Applications Centre, Ahmedabad, India

ABSTRACT: This paper presents a coaxially fed, miniaturized tri-band circularly polarized (CP) antenna with a single layer patch configuration. Broadside radiation is achieved in the L5 band (1.176 GHz), L1 band (1.575 GHz), and S band (2.49 GHz), through the strategic excitation of higher-order modes (TM_{20} and TM_{30}). The antenna design integrates slots and capacitors to reduce the operating frequency, efficiently excite all three modes, and achieve circular polarization within the designated bands. Each frequency band can be independently tuned with minimal effect on the performance of other bands. Moreover, it also facilitates the tuning of polarization sense (from RHCP to LHCP and vice versa) across all three bands. The proposed antenna radiates RHCP at L5, L1, and S bands, with a gain of 1.3 dBi, 1.5 dBi, and 2.7 dBi, respectively. A prototype with dimensions of $0.15\lambda_{L5} \times 0.15\lambda_{L5}$ has been developed and fabricated to validate the antenna's performance.

1. INTRODUCTION

Rapid advancement in the wireless communication with multiple frequencies has led to an increase in the demand of multiband circularly polarized antennas, which can mitigate the Faraday rotation effect and multipath interference [1, 2]. Nowadays, circular polarization is exclusively required for Global Positioning (GPS) System [3, 4], Global Navigation Satellite (GNSS) System [5, 6], Wireless Local Area Networks (WLAN) [7], Radio Frequency Identification (RFID) systems [8]. Many agencies, like the Indian Space Research Organisation, NASA, and the Chinese National Space Administration, are adopting tri-band CP operation, especially for defence purposes, to achieve higher accuracy and avoid any discrepancies during unavoidable situations like war. Moreover, many industries also demand tri-band systems containing GPS and WLAN transceivers.

Various multiband antennas have been developed using stacked patches, metamaterials, fractal geometry, slot and stub loading, modified monopoles, slotted bow ties, and dielectric resonators [9–18]. Stacked patches are commonly used for multiband circularly polarized (CP) antennas [10, 11]; however, they require separate feed layers and multiple patch layers for each band, which increases thickness and bulkiness. Dhara et al. proposed a G-shaped patch with semi-circular slots for tri-band CP operation, but it suffered from an omnidirectional pattern and pattern impurity across all bands [12]. In [13], the authors introduced diagonal and E-plane slots in a double-layer patch antenna to support GPS L1 (1.575 GHz), L2 (1.227 GHz), and DVBH (1.45 GHz). However, this design functions as a dual-band antenna that covers both L1 and L2. Rai et al. used composite right left handed transmission lines to design a compact dual-band antenna. Though the work is commendable, its linear polarization and different patterns in E and H planes limited its application for navigation [14]. A dielectric resonator antenna (DRA) with an Alford loop reported in [15] achieves tri-band CP for GSM, WLAN, and WiMAX but has an omnidirectional pattern and high thickness, limiting its applications. Tharehalli Rajanna et al. proposed a coplanar waveguide (CPW) fed truncated slot patch with split ring resonators (SRRs) to create a tri-band CP antenna [16]; however, it had a significant back lobe at certain frequencies and large dimensions ($1.78\lambda \times 1.78\lambda$). Tan and Chen utilized slots and stub loading on an aperture-coupled patch to achieve tri-band CP [17]. This design increased size due to separate patch and feed layers separated by an air gap, and the aperture coupling led to back radiation, limiting integration with active circuits. Other authors have proposed tri-band CP antennas using annular slots [18] and SRRs, as well as strips loaded rectangular slot antennas [19], but both designs experience high back radiation and interference from nearby metallic components. Reddy and Sarma proposed a fractal based single layer tri-band CP antenna [20], but unwanted nulls were observed in the broadside direction.

A tri-band antenna is necessary for precise vehicle and vessel tracking using Navigation Satellite Systems (NVS). Since these antennas are intended for handheld devices or small gadgets, miniaturization is essential. To the authors' knowledge, single patch layer based tri-band compact CP antenna using slots and capacitors (without increasing antenna size) with the feasibility to tune resonance frequency, as well as the polarization sense, is not available in literature.

In this work, a tri-band CP antenna, having broadside pattern with pattern purity at all three bands, is proposed. Furthermore, a fully backed ground plane facilitates its integration with active circuits, thus catering to the requirement of active antenna for navigation purpose [25, 26]. Electric fields of TM_{20} and TM_{30} modes are tailored to achieve broadside pattern at all

* Corresponding author: Gaurav Kumar (gaurav.kr2802@sac.isro.gov.in).

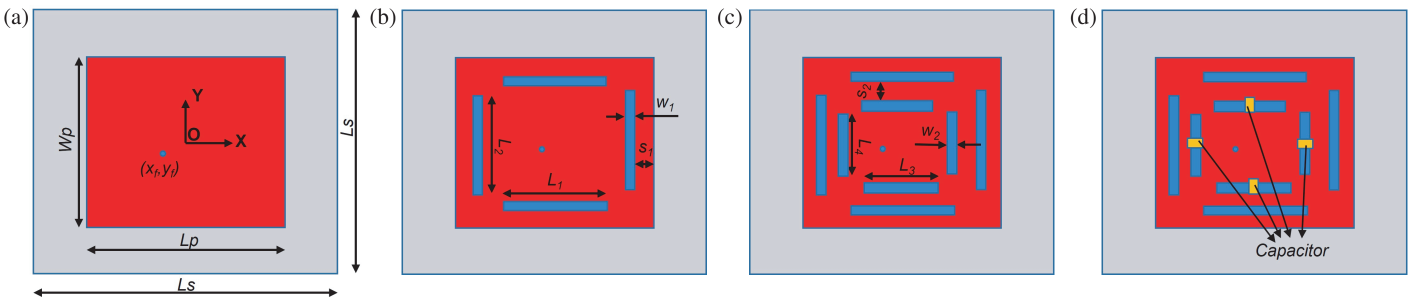

FIGURE 1. Evolution of tri-band antenna. (a) Stage 1. (b) Stage 2. (c) Stage 3. (d) Stage 4.

three bands. The requirement of having simple miniaturized antenna for multiband handheld system as well as vehicles and vessels can also be fulfilled by the proposed miniaturized antenna of size $0.15\lambda_{L5} \times 0.15\lambda_{L5}$ (where λ_{L5} is the free space wavelength at L5 band). The antenna is designed, fabricated, and tested. Section 2 discusses the detailed design process of the proposed antenna. Antenna performance and the comparison of simulated and measured results are shown in Section 3. The paper is finally concluded in Section 4.

2. ANTENNA DESIGN

Multiband operation using a single microstrip patch antenna can be achieved by manoeuvring its higher order modes [21]. It is obtained mainly by four methods — (a) partial loading of metamaterials [22], (b) addition of reflector cum metalens [23], (c) using slots, stubs, and shorting pins [15], and (d) using slots and parasitic elements [24]. The first two methods lead to the increase in antenna size and hamper the efficiency. Although efficiency can be later restored by adding lenses and AMCs, it leads to increase in antenna size and complicates the antenna development. The other two methods use strategic placement of slots, shorts and parasitic elements without increasing the antenna size. TM_{10} has a wide beam broadside pattern whereas TM_{20} mode has a conical pattern, and TM_{30} mode produces broadside with multiple beams. In this manuscript, the last two methods of controlling higher order mode electric fields are wisely utilized to tailor the TM_{20} and TM_{30} modes to achieve broadside radiation in L1, L5, and S bands.

A single square patch antenna is the key module for the proposed tri-band antenna. The evolution of single band CP antenna to tri-band CP antenna is shown in Fig. 1. At first, a coaxially fed square patch is designed to operate at L5 band as shown in Fig. 1(a). A high dielectric substrate is used to miniaturize the antenna. Two degenerate modes TM_{10} and TM_{01} with equal magnitude and 90° phase difference (prime requirement for CP generation) are obtained by diagonal feeding and optimizing length and width of the square patch. Later, two pairs of unequal slots are cut on the patch, parallel to its sides, to tailor the TM_{30} mode, as shown in Fig. 1(b).

Slots are positioned near the radiating edges, where TM_{10} mode has minimal current while TM_{30} mode has significant current. Consequently, the radiation characteristics associated with the TM_{10} mode remain almost unaffected, similar to those of the unperturbed patch. However, the TM_{30} mode current distribution is highly modified, and TM_{30} current circulates around the slots, achieving resonance and broadening the central current distribution to resemble that of the TM_{10} mode. Introducing slots brings down the resonance frequency of both L5 band and S band. Hence, patch and slot dimensions are optimized to achieve the radiation at the intended frequency of L5 and S bands. The length of slots and their positions are adjusted to bring down the resonance in the desired frequency at S band (2.49 GHz). Unequal lengths of the two orthogonal slots (L_1 & L_2) are optimized to achieve circular polarization. Here, L_1 is kept greater than L_2, thus f_{30} leads f_{03} by 90, resulting in RHCP.

These slots also modify the current distribution of TM_{20} mode, as the reduction in the effective patch size prevents complete cancellation of the opposing currents, which is a crucial factor in achieving a null in the broadside direction. Further, another two pairs of orthogonal slots are cut on the patch as shown in Fig. 1(c). Slots are positioned between the center of the antenna and the outer slots significantly modifying the TM_{20} mode current. The inner slot dimensions and their locations play a critical role in TM_{20} mode radiation. The inner slot dimensions and locations are optimized to alter the TM_{20} mode's current density, achieving a broadside pattern. Additionally, incorporating capacitors, as shown in Fig. 1(d), further reduces the TM_{20} mode's resonant frequency, making it suitable for the intended application in L1 band. Similar to the TM_{30} mode slots, uneven lengths of slots L_3 and L_4 are used to achieve circular polarization. Employing slots and capacitors results in the following advantages:

- The resonant frequency of both TM_{20} and TM_{30} modes is significantly lowered.
- The TM_{20} mode's null pattern is transformed into a broadside pattern.
- The TM_{30} mode's triple-lobe radiation pattern becomes similar to that of the TM_{10} mode.

The proposed final antenna is shown in Fig. 2(a). The antenna, providing RHCP at all three bands, is designed on a TMM 13i substrate (with dielectric constant 'ε_r' and thickness 'h') of size 'Ls'. A square patch of length 'L_p' and width 'W_p' is loaded with 8 slots. An outer pair of slots with lengths 'L_1', 'L_2' and width 'W_1' are cut at a distance 'S_1' from edge of the patch, whereas inner slots of length 'L_3' & 'L_4'and width 'W_2' are introduced at 'S_2' distance from the edge of outer slot as

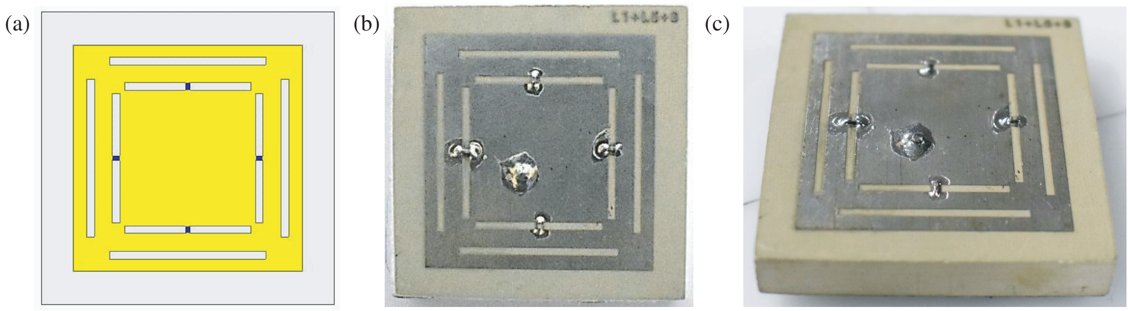

FIGURE 2. (a) Simulation model, fabricated antenna, (b) Top view, and (c) 3D view.

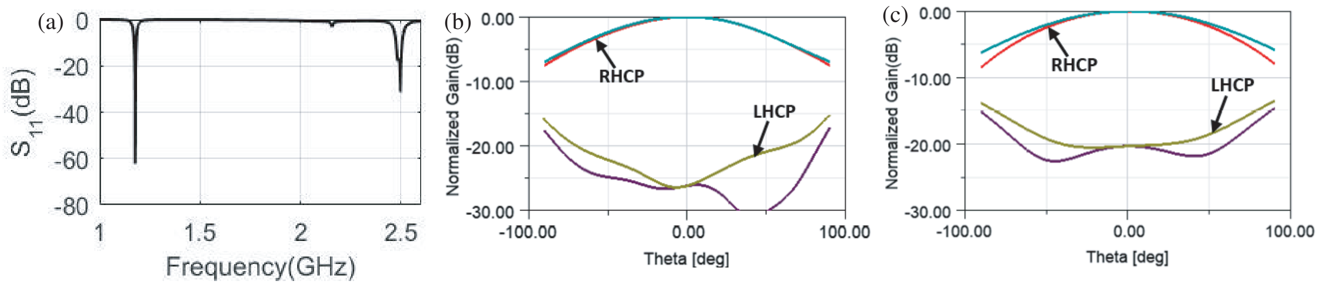

FIGURE 3. Simulated variation of (a) S_{11} with frequency, radiation pattern at (b) L5 band and (c) S band of Stage-2 antenna (L5 + S dual bands).

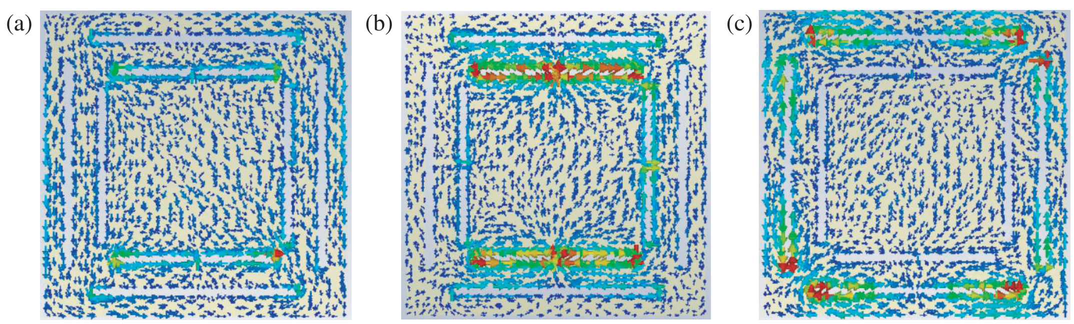

FIGURE 4. Surface current distribution at (a) L5 band (1.176 GHz), (b) L1 band (1.575 GHz), and (c) S band (2.49 GHz).

shown in Fig. 1(c). The antenna is coaxially fed at 'x_f', 'y_f' from centre of the antenna. All the design parameters are tabulated in Table 1.

TABLE 1. Design parameters of the proposed antenna.

Parameter	Value	Parameter	Value
Ls	39 mm	L_3	16.4 mm
L_p	30.3 mm	L_4	16.2 mm
W_p	30.6 mm	W_1	1 mm
X_f	−1.9 mm	W_2	1 mm
Y_f	−2.2 mm	S_1	1.9 mm
L_1	21.0 mm	S_2	2.4 mm
L_2	20.8 mm	***Cap***	2.7 pF

S band and L1 band operation can be tuned individually using outer and inner slots respectively without affecting the L5 band much. Moreover, the patch size can be modified to adjust the antenna performance at L5 band. In addition to that, having separate tuning parameters for each band gives us the freedom to tune the polarization of the antenna at individual band. Any band can be converted from LHCP to RHCP and vice versa just by adjusting the slot length of the orthogonal slots. Theoretically, the proposed antenna has freedom to achieve any of the 8 sets of possible polarization. L_1 and L_2 are adjusted to validate the above statement. The proposed antenna has L_1 longer than L_2 to generate RHCP at L1 band. Making L_2 greater than L_1 allows us to alter the polarization of L1 band from RHCP to LHCP.

3. RESULT AND DISCUSSION

3.1. Simulated Results

All the antenna stages are modelled and simulated in the 3D EM solver Ansys HFSS 2020. As described in the design section, at first a single band CP antenna is designed, and further slots are

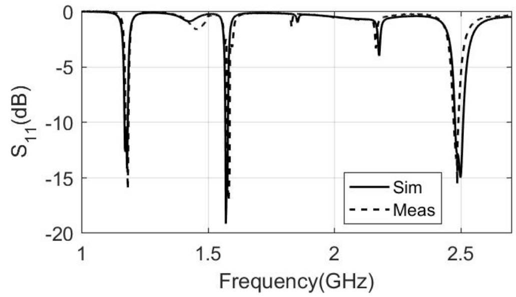

FIGURE 5. Simulated and measured variations of S_{11} with frequency.

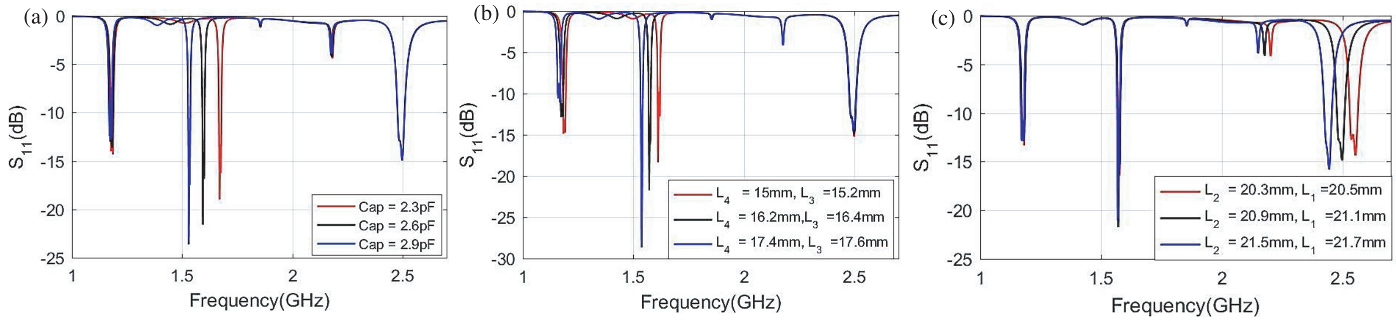

FIGURE 6. Variation of S_{11} with (a) capacitor value, (b) L_3 and L_4, and (c) L_1 and L_2.

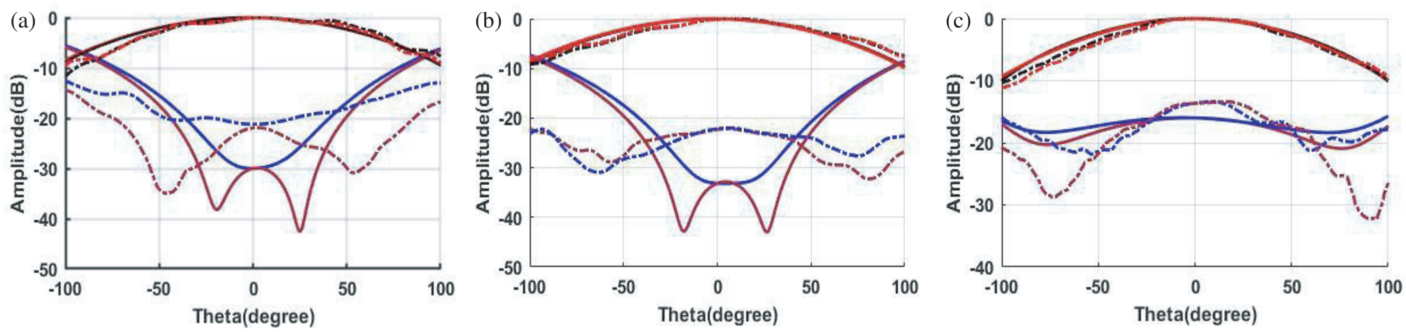

[Simulated RHCP (Ø = 0°), (Ø = 90°), LHCP(Ø = 0°), (Ø = 90°)]

[Measured RHCP (Ø = 0°), (Ø = 90°), LHCP(Ø = 0°), (Ø= 90°)]

FIGURE 7. Simulated and measured radiation patterns at (a) L5 band (1.176 GHz), (b) L1 band (1.575 GHz), and (c) S band (2.49 GHz).

introduced to tailor TM_{30} mode and achieve dual band (L5 + S) CP antenna. The S_{11} and radiation pattern of stage 2 antenna are shown in Fig. 3. Form Fig. 3, it can be deduced that stage 2 antenna attains dual band RHCP operation. The surface current distribution of the proposed (stage 4) antenna, at all three bands, is shown in Fig. 4. It confirms that the outer slots are responsible for S band while the inner slots and capacitor govern the radiation in L1 band. The analyzed S_{11} of the tri-band antenna is shown in Fig. 5, with $S_{11} < -10$ dB bandwidth of 12 MHz, 7 MHz, and 24 MHz at L5, L1, and S band, respectively. As discussed in the previous section, each band of the antenna can be tuned separately without significantly affecting the other bands.

The variation of S_{11} with the capacitor value and length of the slots is shown in Fig. 6. It can be clearly observed from Fig. 6(b) that varying L_1 and L_2 affects only the S band. Similarly, Figs. 6(a) and 6(c) depict the effect of varying the capacitor and inner slot lengths (L_3 and L_4) respectively. We can observe that increasing the capacitor value and slot length reduces the operating frequency of L1 band with a negligible effect on the L5 and S bands. Thus, the proposed antenna has the feature to independently control the operating frequencies in each band.

Figure 7 shows the simulated radiation pattern at the L5, L1, and S bands, respectively. Fig. 8 illustrates the analyzed axial ratios of the antenna, 0.5 dB, 0.1 dB, and 2 dB at L5, L1, and S bands, respectively. Antenna radiates RHCP with gains of 1.3 dBi, 1.5 dBi, and 2.7 dBi at L5, L1, and S bands, respectively, as shown in Fig. 9.

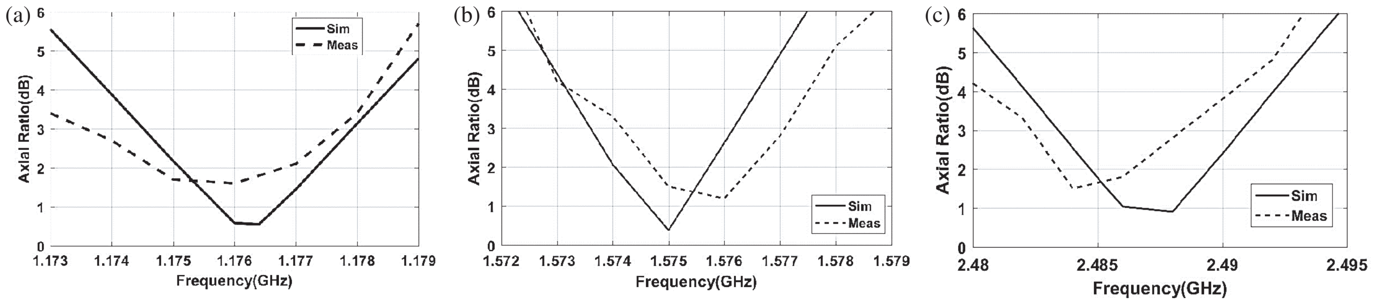

FIGURE 8. Axial ratio at (a) L5 band (1.176 GHz), (b) L1 band (1.575 GHz), and (c) S band (2.49 GHz).

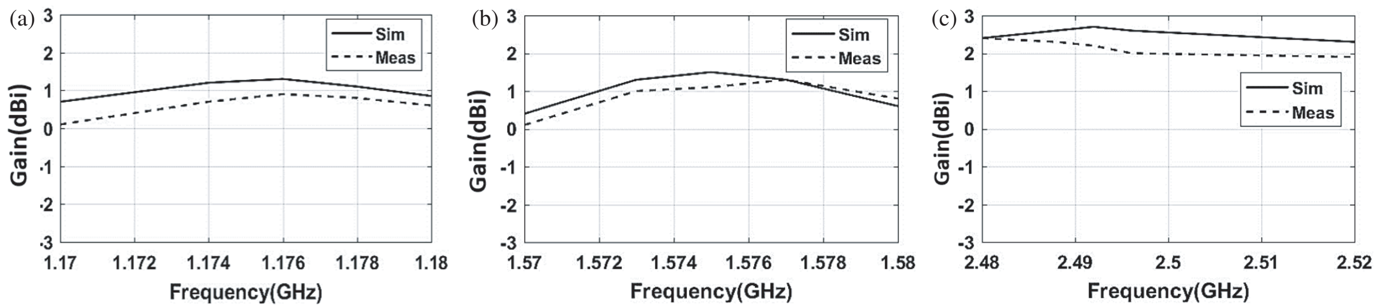

FIGURE 9. Gain at (a) L5 band (1.176 GHz), (b) L1 band (1.575 GHz), and (c) S band (2.49 GHz).

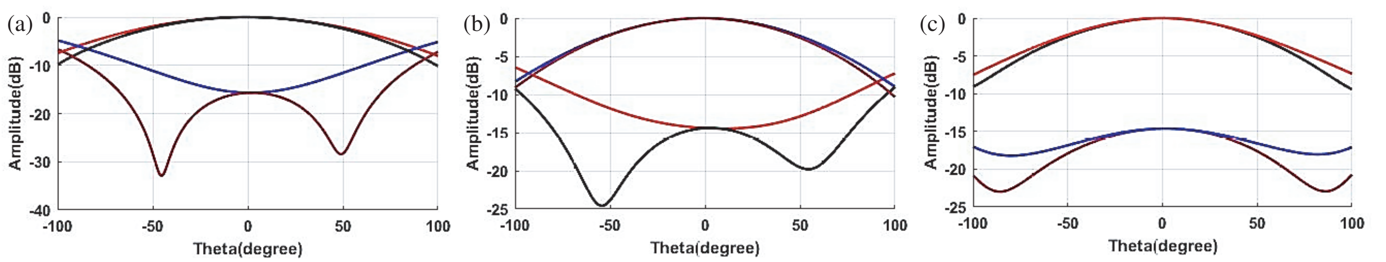

[Simulated Co pol (Ø = 0°), (Ø = 90°), Cross pol(Ø = 0°), (Ø = 90°)]

FIGURE 10. Radiation pattern of antenna (with modified L1 band polarization, i.e., LHCP at L1band and RHCP at L5 and S band). (a) L5 band (1.176 GHz), (b) L1 band (1.575 GHz), and (c) S band (2.49 GHz).

3.2. Measured Results

The antenna is fabricated using photolithography in Space Applications Centre, Ahmedabad, and the fabricated antenna is shown in Fig. 2(b) and Fig.2(c). Here, commercially available 0402 package, murata capacitors 'GJM1555C1H2R0WB01D' (2.7 pF $\pm$ 0.05 pF) are mounted on the inner slots.

The S_{11} of the fabricated antenna is measured using a vector network analyzer, and the performance is shown in Fig. 5. It is clear that the measured S_{11} closely matches the simulated one. The antenna radiation pattern is measured in the tapered anechoic chamber of Space Application Centre, Ahmedabad. Measured radiation patterns are plotted in Fig. 7, verifying that the antenna radiates RHCP at all three bands (L5, L1, and S band). Fig. 8 and Fig. 9 show the simulated and measured axial ratios and gains, respectively, at all three frequency bands. Gains of 0.9 dBi, 1.3 dBi, and 2.4 dBi are achieved at L5, L1, and S bands, respectively. Axial ratio of less than 3 dB is achieved at all three bands.

Figures 5–9 demonstrate that the simulated and measured performances are in close agreement. Minor variations can be attributed to the capacitor parasitics and fabrication tolerances.

The proposed antenna also has the capability to tune the polarization from RHCP to LHCP. Values of L_3 and L_4 are reversed to produce LHCP at the L1 band, and the performance is shown in Fig. 10. It is confirmed that by modifying L_3 and L_4, the antenna radiates LHCP at L1 band and RHCP at L5 and S bands. Hence, it can be concluded that the polarization of L1 band is reversed, while the polarization as well as the performance of L5 and S bands are preserved. Additionally, L_1 and L_2 can be tuned to convert the antenna polarization from RHCP to LHCP and vice versa at the S band. The comparison of this work with prior works are tabulated in Table 2. The proposed antenna provides a compact viable option for multiband applications, especially for GNSS and Wi-Fi. Although this structure has a narrow bandwidth, it is an ideal option for low cost navigation applications, where small bandwidth is re-

TABLE 2. Comparison with the prior works.

Ref.	Size	Central frequency	Gain (dBi)	Polarization tunability
21	$0.72\lambda^2$	2.45,3.35, 4.35	7.5, 8.7, 8.7	Yes
22	$0.5\lambda^2$	1.22,1.57,2.31	4, 4.6, 5.7	No
26	$0.3\lambda^2$	1.83, 2.5,3.1	2.7,4.2,3.5	Yes
27	$0.95\lambda^2$	2.63,3.45, 4.65	6.6,3.9,6.7	No
28	$0.4\lambda^2$	2.45, 3.4, 5.8	6.5, 4.5, 3	No
This work	$0.15\lambda^2$	1.176,1.575,2.49	1.3,1.5,2.7	Yes

quired, and size is crucial. Most vessels and vehicles use these kinds of miniaturized antennas for navigation. Moreover, the bandwidth and gain of the proposed antenna can be increased by reducing the dielectric constant of the substrate and increasing the size of the ground (either by mounting it on a big ground plane or increasing antenna size).

4. CONCLUSION

A miniaturized tri-band circularly polarized (CP) antenna has been designed, developed, and tested. The coaxially fed single substrate patch features eight slots and four capacitors, radiating right-hand circular polarization (RHCP) at the L5, L1, and S bands. Slot and capacitor loading is employed to manipulate higher-order modes and achieve multiband operation. Results demonstrate that higher-order modes, such as the TM_{20} mode with a null at the center and the TM_{30} mode with multiple lobes, can be modified to produce a broadside pattern similar to that of the TM_{10} mode. Moreover, the antenna includes separate parameters to tune all three frequencies, enabling modifications in the frequency of operation and adjustments in polarization sense (i.e., from RHCP to LHCP and vice versa).

ACKNOWLEDGEMENT

The authors thank Shri. N. M. Desai, Director, SAC for his enormous support and motivation to carry out this work. The authors also wish to thank engineers of Antenna System Area (ASA) for their help in development and pattern measurement of the antenna.

REFERENCES

[1] Lee, C.-H. and Y.-H. Chang, "An improved design and implementation of a broadband circularly polarized antenna," *IEEE Transactions on Antennas and Propagation*, Vol. 62, No. 6, 3343–3348, Jun. 2014.

[2] Han, R.-C., S.-S. Zhong, and J. Liu, "Design of circularly-polarized dielectric resonator antenna with wideband feed network," in *Proceedings of 2014 3rd Asia-Pacific Conference on Antennas and Propagation*, 48–50, Harbin, China, Jul. 2014.

[3] Sun, C., H. Zheng, and Y. Liu, "Analysis and design of a low-cost dual-band compact circularly polarized antenna for GPS application," *IEEE Transactions on Antennas and Propagation*, Vol. 64, No. 1, 365–370, Jan. 2016.

[4] Cai, Y.-M., K. Li, Y.-Z. Yin, and X. Ren, "Dual-band circularly polarized antenna combining slot and microstrip modes for GPS with HIS ground plane," *IEEE Antennas and Wireless Propagation Letters*, Vol. 14, 1129–1132, 2015.

[5] Zhang, H., Y. Guo, and G. Wang, "A design of wideband circularly polarized antenna with stable phase center over the whole GNSS bands," *IEEE Antennas and Wireless Propagation Letters*, Vol. 18, No. 12, 2746–2750, Dec. 2019.

[6] Zhang, Y.-Q., X. Li, L. Yang, and S.-X. Gong, "Dual-band circularly polarized annular-ring microstrip antenna for GNSS applications," *IEEE Antennas and Wireless Propagation Letters*, Vol. 12, 615–618, 2013.

[7] Weng, W.-C., J.-Y. Sze, and C.-F. Chen, "A dual-broadband circularly polarized slot antenna for WLAN applications," *IEEE Transactions on Antennas and Propagation*, Vol. 62, No. 5, 2837–2841, May 2014.

[8] Chen, X., G. Fu, S.-X. Gong, Y.-L. Yan, and W. Zhao, "Circularly polarized stacked annular-ring microstrip antenna with integrated feeding network for UHF RFID readers," *IEEE Antennas and Wireless Propagation Letters*, Vol. 9, 542–545, 2010.

[9] Sharma, A., G. Das, S. Gupta, and R. K. Gangwar, "Quad-band quad-sense circularly polarized dielectric resonator antenna for GPS/CNSS/WLAN/WiMAX applications," *IEEE Antennas and Wireless Propagation Letters*, Vol. 19, No. 3, 403–407, Mar. 2020.

[10] Wang, S., L. Zhu, and W. Wu, "3-D printed inhomogeneous substrate and superstrate for application in dual-band and dual-CP stacked patch antenna," *IEEE Transactions on Antennas and Propagation*, Vol. 66, No. 5, 2236–2244, May 2018.

[11] Chung, K. L. and A. S. Mohan, "A circularly polarized stacked electromagnetically coupled patch antenna," *IEEE Transactions on Antennas and Propagation*, Vol. 52, No. 5, 1365–1369, May 2004.

[12] Dhara, R., M. Sarkar, T. K. Dey, and S. K. Jana, "A tri-band circularly polarized G-shaped patch antenna for wireless communication application," in *2018 International Conference on Computing, Power and Communication Technologies (GUCON)*, 992–996, Greater Noida, India, Sep. 2018.

[13] Zahid, M. N., J. Jiang, N. Ashraf, and M. S. Nazirb, "Tri-band circularly polarized micro-strip patch antenna for GPS and DVB-h applications," in *2019 16th International Bhurban Conference on Applied Sciences and Technology (IBCAST)*, 1029–1033, Islamabad, Pakistan, Jan. 2019.

[14] Rai, J. K., K. Anuragi, N. Mishra, R. Chowdhury, S. Kumar, and P. Ranjan, "Dual-band miniaturized composite right left handed transmission line ZOR antenna for microwave communication with machine learning approach," *AEU — International Journal of Electronics and Communications*, Vol. 176, 155120, 2024.

[15] Cheng, C., F. Zhang, Y. Yao, and F. Zhang, "Triband omnidirectional circularly polarized dielectric resonator antenna with

top-loaded alford loop," *International Journal of Antennas and Propagation*, Vol. 2014, No. 1, 797930, 2014.

[16] Tharehalli Rajanna, P. K., K. Rudramuni, and K. Kandasamy, "Compact triband circularly polarized planar slot antenna loaded with split ring resonators," *International Journal of RF and Microwave Computer-Aided Engineering*, Vol. 29, No. 12, e21953, 2019.

[17] Tan, Q. and F.-C. Chen, "Triband circularly polarized antenna using a single patch," *IEEE Antennas and Wireless Propagation Letters*, Vol. 19, No. 12, 2013–2017, Dec. 2020.

[18] Liao, W., Q.-X. Chu, and S. Du, "Tri-band circularly polarized stacked microstrip antenna for GPS and CNSS applications," in *2010 International Conference on Microwave and Millimeter Wave Technology*, 252–255, Chengdu, China, May 2010.

[19] Paul, P. M., K. Kandasamy, and M. S. Sharawi, "A triband circularly polarized strip and SRR-loaded slot antenna," *IEEE Transactions on Antennas and Propagation*, Vol. 66, No. 10, 5569–5573, Oct. 2018.

[20] Reddy, V. V. and N. V. S. N. Sarma, "Triband circularly polarized koch fractal boundary microstrip antenna," *IEEE Antennas and Wireless Propagation Letters*, Vol. 13, 1057–1060, 2014.

[21] Zhang, J.-D., L. Zhu, N.-W. Liu, and W. Wu, "Dual-band and dual-circularly polarized single-layer microstrip array based on multiresonant modes," *IEEE Transactions on Antennas and Propagation*, Vol. 65, No. 3, 1428–1433, Mar. 2017.

[22] Xiong, J., X. Lin, Y. Yu, M. Tang, S. Xiao, and B. Wang, "Novel flexible dual-frequency broadside radiating rectangular patch antennas based on complementary planar ENZ or MNZ metamaterials," *IEEE Transactions on Antennas and Propagation*, Vol. 60, No. 8, 3958–3961, 2012.

[23] Chatterjee, A. and S. K. Parui, "Performance enhancement of a dual-band monopole antenna by using a frequency-selective surface-based corner reflector," *IEEE Transactions on Antennas and Propagation*, Vol. 64, No. 6, 2165–2171, Jun. 2016.

[24] Huang, C.-Y., H.-F. Tsai, M.-H. Lin, and P.-Y. Chiu, "Chip-capacitor loaded dual-band microstrip antenna," in *IWAT 2005. IEEE International Workshop on Antenna Technology: Small Antennas and Novel Metamaterials, 2005.*, 227–229, Singapore, Mar. 2005.

[25] Wang, Z., H. Liu, S.-J. Fang, and Y. Cao, "A low-cost dual-wideband active GNSS antenna with low-angle multipath mitigation for vehicle applications," *Progress In Electromagnetics Research*, Vol. 144, 281–289, 2014.

[26] Go, J.-G. and J.-Y. Chung, "Active GNSS antenna implemented with two-stage LNA on high permittivity substrate," *Journal of Electrical Engineering and Technology*, Vol. 13, No. 5, 2004–2010, 2018.